

## Taranakite from the Onino-Iwaya Limestone Cave at Hiroshima Prefecture, Japan: A New Occurrence

TOSHIRO SAKAE, AND TOSHIO SUDO

*Geological and Mineralogical Institute, Faculty of Science,  
Tokyo University of Education, Otsuka, Bunkyo-ku, Tokyo, Japan*

### Abstract

Taranakite— $H_{7.08}K_{1.97}(Al,Fe)_{4.98}(PO_4)_{8.00} \cdot 19.7H_2O$ —occurs as aggregates of fine powdery crystals intercalated in clay sediments in the Onino-Iwaya limestone cave at Hiroshima Prefecture, Japan. Cell dimensions of the mineral determined by least-squares method on the basis of a hexagonal six-layer structure are  $a = 8.718(2) \text{ \AA}$  and  $c = 95.18(3) \text{ \AA}$ . Three endothermic DTA peaks occur at 120°C, 180°C, and 990°C, and an exothermic peak at 550°C. The TG curve shows a weight loss of 31.1 percent in the temperature interval from 100 to 200°C. The observed phase changes may be summarized as follows: (natural sample) 120°C, a partially dehydrated form; 180°C, a non-crystalline state; 550°C, a recrystallized state; 990°C, a transformed state. Taranakite may be formed as bat guano in clay sediments takes up potassium and aluminum ions dissolved from the clays.

### Introduction

A mineral that was described and given the name taranakite by Hector and Skey (1865) has been found successively from caves in France (Gautier, 1894), Italy (Casorio, 1904), Algeria, New South Wales, the island of Reunion in the Indian Ocean (Palache, Berman, and Frondel, 1957), and Pig Hole Cave, Giles County, Virginia (Murray and Dietrich, 1956). Gautier (1894) and Casorio (1904) named their minerals minervite and palmerite respectively, but these were proved later to be identical to taranakite (Bannister and Hutchingson, 1947).

This present paper reports the mode of occurrence and some mineralogical properties of taranakite recently found in the Onino-Iwaya limestone cave at Hiroshima Prefecture, Japan.

### Mode of Occurrence

Taranakite occurs as  $20 \times 20 \times 1 \text{ cm}$  (*ca*) lenticular associated with a minor amount of apatite aggregates of white powdery crystals intercalated in clay sediments at 2 to 3 cm below the present surface. The mode of occurrence of taranakite resembles that of bat guano in the cave. Within the surrounding clay sediments, which consist of mica, chlorite, halloysite, montmorillonite, and kaolinite, taranakite is scarce except below the taranakite lenses.

### Mineralogical Properties

#### Specific Gravity

Fine crystals of taranakite, freed from impurity by hand picking with a tweezers under a binocular,

proved soluble in hydrochloric acid but not in water. Their specific gravity, measured using a pycnometer, is 2.06 and thus close to the calculated value (2.11) given by Smith and Brown (1959), and to the value (2.12) calculated from the present lattice parameters and chemical composition. Crystal sizes are too small (less than 0.01 mm) to provide reliable optical properties.

TABLE 1. Chemical Analyses of Taranakite

	weight %		
	1	2	3
K <sub>2</sub> O	7.09	9.87	10.53
Na <sub>2</sub> O	tr.	nd.	-
CaO	tr.	-	-
MgO	tr.	-	-
MnO	nd.	-	-
Al <sub>2</sub> O <sub>3</sub>	19.03	18.65	18.99
Fe <sub>2</sub> O <sub>3</sub>	0.42	nd.	-
P <sub>2</sub> O <sub>5</sub>	42.32	42.39	42.30
H <sub>2</sub> O (+)	nd.	nd.	4.03*
H <sub>2</sub> O (-)	31.10	29.51	24.15
Rem.	tr.	nd.	-
Total	99.96	100.42	100.00

1: Present sample. 2: Synthetic sample from chemicals. 3: Ideal composition;  $H_6K_3Al_5(PO_4)_8 \cdot 18H_2O$ .  
\*: H<sub>2</sub>O calculated from H.  
(Analyst, T.Sakae)

TABLE 2. X-ray Powder Diffraction Patterns

<i>h</i>	<i>k</i>	<i>l</i>	1 <i>d(calc)</i>	2 <i>d(obs)</i>	I/I <sub>0</sub>	3 <i>d(obs)</i>	I/I <sub>0</sub>	4 <i>d(obs)</i>	I/I <sub>0</sub>	5 <i>d(obs)</i>	I/I <sub>0</sub>	6 <i>d(obs)</i>	I/I <sub>0</sub>	7 <i>d(obs)</i>	I/I <sub>0</sub>	8 <i>d(obs)</i>	I/I <sub>0</sub>
0	0	6	15.868	16.01	100	15.92	100	16.1	100	14.4	100					7.05	6
0	0	12	7.934	7.957	21	7.949	12	7.97	22	7.47	100					6.06	4
0	1	2	7.457	7.487	15	7.474	3	7.47	38	6.97	60	5.72	44			5.71	45
1	0	4	7.196	7.225	3	7.237	1	7.20	6	6.56	20	5.22	7			5.22	4
1	0	10	5.916	5.930	10	5.926	3	5.92	9	6.15	20	4.37	77	4.42	40	4.36	44
0	1	14	5.053	5.068	2	5.056	1			5.60	60	4.14	100	4.16	100	4.13	62
1	0	16	4.673	4.683	3	4.673	1	4.51	6	4.35	60					4.09	100
1	1	0	4.359	4.366	6	4.358	1	4.35	6	4.31	60	3.87	54	3.90	22	3.86	54
1	1	3	4.318	4.322	10	4.322	2	4.31	8	4.16	50					3.74	3
1	1	6	4.203	4.206	1	4.208	1	4.27	6	3.69	30					3.69	3
0	1	20	4.027	4.029	5	4.026	1			3.42	90	3.60	6	3.62	3	3.61	4
1	1	12	3.820	3.824	25	3.821	5	3.82	18	3.16	40	3.53	5				
1	0	22	3.754	3.753	9	3.754	2	3.75	7	3.05	30	3.49	6			3.50	6
2	0	8	3.598	3.596	13	3.594	3	3.59	9	2.92	40	3.31	18			3.33	18
1	1	18	3.364	3.365	7	3.363	1			2.81	40					3.29	7
2	0	14	3.301	3.302	8	3.299	2	3.30	7	2.78	40					3.17	8
0	2	16	3.188	3.191	7	3.186	2	3.18	6	2.69	30	3.08	12			3.08	7
0	0	30	3.174	3.173	7	3.171	2			2.66	20	3.03	15	3.04	5	3.04	13
1	1	21	3.142	3.143	19	3.140	5	3.14	8	2.36	20	2.98	14			2.99	10
2	0	20	2.958	2.957	3	2.955	1			2.30	20	2.94	40			2.94	34
1	1	24	2.934	2.931	3	2.930	1			2.09	20	2.90	67			2.90	52
0	2	22	2.845	2.844	9	2.842	2	2.84	6	2.06	10					2.77	3
1	2	5	2.822	2.823	10	2.820	2	2.82	8	2.03	20					2.69	2
2	1	7	2.793	2.794	3	2.791	1			1.96	10	2.58	5			2.59	4
2	1	10	2.741	2.738	6	2.739	1	2.74	4	1.88	10	2.55	5	2.56	26	2.56	7
1	2	11	2.710	2.710	2	2.708	1					2.53	16			2.51	14
0	0	36	2.645	2.644	9	2.643	3	2.64	6							2.42	3
2	0	26	2.628	2.628	10	2.628	2									2.38	8
2	1	16	2.573	2.572	3	2.571	1					2.36	4			2.35	3
1	2	17	2.543	2.542	2	2.539	1	2.53	4			2.32	4			2.34	3
0	3	6	2.486	2.485	1	2.481	1	2.47	2			2.31	6			2.31	3
3	0	12	2.399	2.398	6	2.397	1	2.39	4			2.28	6			2.27	3
1	2	23	2.349	2.348	2	2.345	1					2.26	5				
0	0	42	2.267	2.266	2	2.266	1	2.26	2							2.23	3
2	2	0	2.179	2.173	1							2.16	4			2.16	3
1	2	29	2.154	2.151	1	2.150	1					2.11	4			2.11	5
3	0	24	2.125	2.123	2	2.120	1					2.09	4	2.08	5	2.09	6
2	1	31	2.090	2.094	2	2.090	1	2.10	2			2.06	6			2.06	4
1	3	7	2.070	2.069	5	2.070	1	2.07	4			2.02	3				
3	0	27	2.048	2.047	2							1.996	5			1.993	2

1 = Calculated spacings; 2 = Present sample; 3 = Synthetic sample from chemicals; 4 = Synthetic sample from micas; 5 = Product after heating at 120°C for 15 minutes; 6 = Product after heating at 600°C for one hour; 7 = Product kept at 1000°C for 40 minutes; 8 = Product after heating at 1000°C for 40 minutes. Patterns 2, 3, 4 are untreated samples X-rayed at room temperature, whereas 5, 6, and 8 are heat treated samples X-rayed at room temperature, 7 is taken above room temperature (at 1000°C).

### Chemical Composition

Using a 0.1 g sample, the chemical constituents such as Fe<sup>3+</sup>, Al<sup>3+</sup>, Ca<sup>2+</sup>, Mg<sup>2+</sup>, Mn<sup>2+</sup>, and PO<sub>4</sub><sup>3-</sup> were separated from one another by ion-exchange resins (Oki *et al.*, 1962) and analyzed by chelate-titration. Chemical constituents such as Na<sup>+</sup> and K<sup>+</sup> were analyzed by flame photometer, and SO<sub>4</sub><sup>2-</sup> was analyzed by the usual gravimetric methods. The results are shown in Table 1.

Chemical formulas of taranakite have been calculated on the basis of (PO<sub>4</sub>)<sub>7</sub>, (PO<sub>4</sub>)<sub>5</sub>, (PO<sub>4</sub>)<sub>3</sub>, or (PO<sub>4</sub>)<sub>8</sub> by Murray and Dietrich (1956), Haseman, Lehr, and Smith (1951), Bannister and Hutchingson

(1947), and Smith and Brown (1959) respectively. We used (PO<sub>4</sub>)<sub>8</sub> as the basis because, in the present case, the ion ratios so calculated were, as a rule, closer to integers than those calculated on the other bases. The resulting chemical formula



is close to that presented by Smith and Brown (1959) except for more hydrogen and less potassium, this suggesting substitution of H for K.

### X-ray Crystallography

X-ray powder diffraction patterns (Table 2, col. 2) obtained using a RIGAKU diffractometer (CuKα,

1.5418 Å) agree with those reported by Haseman *et al* (1951) and Murray and Dietrich (1956). Haseman *et al* (1951) and Smith and Brown (1959) suggested that their patterns of taranakite could be reasonably indexed on the basis of a hexagonal six-layer structure. Our pattern was indexed on the basis of the lattice parameters given by Smith and Brown (1959). Using these indices and observed spacings, the lattice parameters were refined to  $a = 8.718(2)$  Å and  $c = 95.18(3)$  Å by least-squares method. The computation was carried out on a MELCOM 7500 computer at the Tokyo University of Education. On the basis of these refined parameters, final indices and calculated spacings were obtained as shown in Table 2, columns 1 and 2.

#### Thermal Study

DTA and TG curves were obtained in air with RIGAKU thermoflex under the following conditions: thermocouple, Pt-PtRh; reference,  $\text{Al}_2\text{O}_3$ ; mean heating rate,  $10^\circ\text{C}/\text{min.}$ ; sensitivity (DTA),  $\pm 250 \mu\text{V}$ ; sensitivity (TG), 10 mg; sample weight, 25.66 mg (Fig. 1-B). Three endothermic peaks occur at  $120^\circ\text{C}$ ,  $180^\circ\text{C}$ , and  $990^\circ\text{C}$ . The first two endotherms accompany a weight loss of 31.1 percent, but the last one shows no weight change. On cooling, the DTA curve shows a complementary peak corresponding to the last endotherm. An exothermic peak occurs at  $550^\circ\text{C}$  without weight change.

The heat-treated products were studied in the following two ways: (a) The sample was heated at various high temperatures for short durations of time (15 min. to 1 hour) and then quenched to room temperature. X-ray powder diffraction patterns of the quenched sample were recorded. (b) X-ray powder diffraction patterns were recorded at temperature with a high-temperature X-ray diffractometer. The X-ray powder pattern of the heat-treated product at  $120^\circ\text{C}$  (Table 2, col. 5) differed slightly from that of unheated sample. The high-temperature pattern at  $120^\circ\text{C}$  appears the same as that of the quench product (Table 2, col. 5). This suggests that the modification is due to a sluggish phase transformation. The product heat-treated at  $180^\circ\text{C}$  is a non-crystalline state which recrystallizes at about  $550^\circ\text{C}$  as shown by an exothermic peak in the DTA curve. High-temperature X-ray powder patterns show that the  $d$  values of the reflections progressively increase as temperature is increased from  $600^\circ\text{C}$  to  $1000^\circ\text{C}$ , and that the three main reflections at 5.72 Å, 2.94 Å, and 2.90 Å have disappeared at  $1000^\circ\text{C}$ . However, patterns of the quench product show that the above

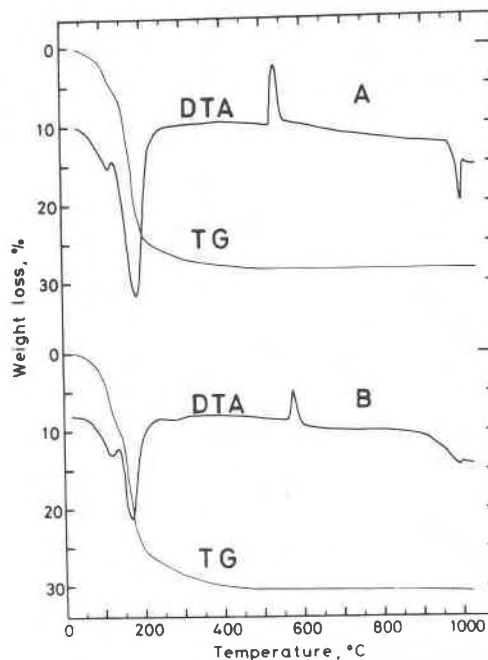


FIG. 1. DTA and TG analyses of taranakite. A: Taranakite synthesized from  $\text{AlCl}_3 \cdot 6\text{H}_2\text{O}$  and  $\text{H}_3\text{PO}_4$  with KOH buffer, pH 3,  $60^\circ\text{C}$ . B: Natural sample.

modifications are reversible. This suggests that these modifications are due to a rapid phase transformation.

#### Infrared Absorption Spectra

An infrared absorption spectrum of taranakite (Fig. 2-A) was obtained with JASCO IR-2 using KBr disk. The spectrum agrees with those reported by Arlidge *et al* (1963). We could not confirm the occurrence of the absorption peak at  $1600 \text{ cm}^{-1}$  which Arlidge *et al* (1963) reported and attributed to the vibration of ammonium ions.

#### Electron Microscopic Observation

An electron micrograph of taranakite shows thin platy crystals of hexagonal shape and 2 to 3  $\mu$  in average diameter. These easily convert to a non-crystalline state under the electron beam.

#### Synthesis of Taranakite

It has been reported that taranakite can be synthesized from chemicals or micas (Haseman *et al*, 1950, 1951). We synthesized taranakite by the methods reported by these workers. The synthetic taranakite is similar to the natural sample with regard to chemical composition (Table 1, col. 2), X-ray powder diffraction pattern (Table 2, cols. 3 and 4),

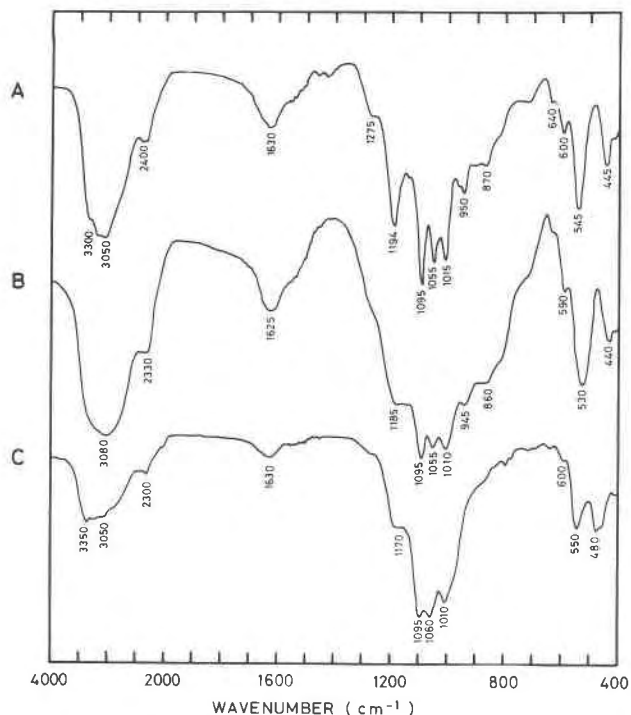


FIG. 2. Infrared absorption spectra of taranakite. A: Natural sample. B: Taranakite synthesized from  $\text{AlCl}_3 \cdot 6\text{H}_2\text{O}$  and  $\text{H}_3\text{PO}_4$  with KOH buffer, pH 3,  $60^\circ\text{C}$ . C: Taranakite synthesized from Matsumae mica and  $\text{H}_3\text{PO}_4$  with KOH buffer, pH 3,  $60^\circ\text{C}$ .

DTA and TG curves (Fig. 1-A), and infrared absorption spectra (Fig. 2-B, C).

### Conclusion

On the basis of the above data, the thermal change of taranakite may be summarized as follows: (natural sample)  $120^\circ\text{C}$ , a partially dehydrated form;  $180^\circ\text{C}$ , a non-crystalline state;  $550^\circ\text{C}$ , a recrystallized state;  $990^\circ\text{C}$ , a transformed state. The endotherm at  $120^\circ\text{C}$  represents a partial dehydration, the one at  $180^\circ\text{C}$  represents a disintegration of the dehydrated structure, the exotherm at  $550^\circ\text{C}$  represents a recrystallization, and the endotherm at  $990^\circ\text{C}$  represents a transformation of this recrystallized state. The partially dehydrated form corresponds to the "lower hydrate form" reported by Haseman *et al* (1951), and the phase transformation occurring at  $990^\circ\text{C}$  apparently relates the  $T_3$  and  $T_4$  phases reported by Murray and Dietrich (1956).

The mode of occurrence and the result of synthesis

suggest that taranakite may be formed by a chemical reaction between clays and phosphoric acid (Stout, 1939). Because the mode of occurrence of the present taranakite resembles that of bat guano, chemical reaction between phosphoric acid in bat guano and the potassium and aluminum ions dissolved from surrounding clays may play an important role in the formation of the present taranakite.

### Acknowledgments

One of the authors (T. Sakae) wishes to thank Professor M. Okubo of Shimane University for his suggestions and helpful advice in the course of the cave research. The authors are indebted to Dr. S. Shimoda and the members of the Mineralogical Institute, Tokyo University of Education, for their support and for critical discussions. A part of the expense of the study was defrayed by a Grant-in-Aid for Science Research of the Ministry of Education.

### References

- ARLIDGE, E. Z., V. C. FARMER, B. D. MITCHELL, AND W. A. MITCHELL (1963) Infra-red, X-ray, and thermal analysis of some aluminum and ferric phosphates. *J. Appl. Chem.* **13**, 17-27.
- BANNISTER, F. A., AND G. E. HUTCHINGSON (1947) The identity of minervite and palmerite with taranakite. *Mineral. Mag.* **28**, 31-35.
- CASORIO (1904) *Acc. Georgofili, Att.*, **1**, July 3. Ref. in Palache *et al*, *Dana's System of Mineralogy*, 7th ed., **2** (1957).
- GAUTIER (1894) V-Minervite; nouveau phosphate d'alumine hydrate. *Ann. Mines*, **5**, 23-28.
- HASEMAN, J. F., E. H. BROWN, AND C. D. WHITT (1950) Some reactions of phosphate with clays and hydrous oxides of iron and aluminum. *Soil Science*, **70**, 257-271.
- , J. R. Lehr, and J. P. Smith (1951) Mineralogical character of some iron and aluminum phosphates containing potassium and ammonium. *Soil Sci. Soc. Proc. Am. p.* 76-84.
- HECTOR AND SKEY (1865) *Rpts. of Jurors, New Zealand Exped.*, p. 423. Ref. in Palache *et al*, *Dana's System of Mineralogy*, 7th ed., vol. **2** (1957).
- MURRAY, J. W., AND R. V. DIETRICH (1956) Brushite and taranakite from Pig Hole Cave, Giles county, Virginia. *Am. Mineral.* **41**, 616-626.
- OKI, Y., S. OKI, H. SHIBATA, AND Y. SAKAKIBARA (1962) Analysis of rocks by means of ion-exchange resins and chelate-titration method (2). *J. Geol. Soc. Japan*, **68**, 329-333.
- PALACHE, C., H. BERMAN, AND C. FRONDEL (1957) *Dana's System of Mineralogy*, 7th ed., vol. **2**, John Wiley and Sons, New York.
- SMITH, J. P., AND W. E. BROWN (1959) X-ray studies of aluminum and iron phosphates containing potassium or ammonium. *Am. Mineral.* **44**, 138-142.
- STOUT, P. R. (1939) Alterations in the crystal structure of clay minerals as a result of phosphate fixation. *Soil Sci. Soc. Proc. Am. p.* 177-182.

Manuscript received, May 13, 1974; accepted for publication, October 25, 1974.